REAL-TIME DISPLACEMENT AND TILT ANALYSIS BY A SPECKLE TECHNIQUE USING $Bi_{12}SiO_{20}$-CRYSTALS

H.J. TIZIANI, K. LEONHARDT and J. KLENK
Institut für Technische Optik der Universität Stuttgart, 7000 Stuttgart 80, Fed. Rep. Germany

Received 9 April 1980
Revised manuscript received 9 June 1980

Storage of speckle pattern in real time by means of $Bi_{12}SiO_{20}$-crystals will be reported. Applying the double exposure technique, deformations, displacements as well as tilts can be analysed. The novel speckle technique displays the Young'-interference fringes in quasi real time.

1. Introduction

Speckle photography is becoming an important method for deformation, displacement and tilt measurements. The technique will be even more attractive to the engineer when its application is in real time. Therefore, the developing process of speckle photography and the subsequent optical Fourier transformation of the photographs will be replaced.

Bismuth silicon oxyde $Bi_{12}SiO_{20}$, has electrical and electrooptical properties which make it attractive for dynamic holography and speckle applications. The basic principle for application of the crystal to holographic storage, double-exposure and time average interferometry of transparent or mirror like structures was reported [1,2].

Upon readout of the hologram at the same wavelength the reconstructing light beam erases the stored information. Therefore, by the double-exposure technique, the second exposure partially erases the stored information. By the reconstruction, the resulting image with the interference fringes superimposed, can be stored by means of a video storage device or on film.

For real time holography and holographic interferometry the BSO crystal is biased with a transverse electric field E_0 in the 110 crystallographic direction. When the crystal is illuminated with spatially structured illumination in the $\bar{1}10$ direction, a space-charge field is built up. A photoinduced space-charge density due to the difference between the distribution of trapped electrons and holes is generated [1]. The resultant space-charge field changes the refractive index of the crystal via linear electrooptic effect. A phase volume hologram is created. Floading with uniform illumination leads to the erasure of the stored information by space-charge relaxation. Consequently, reading out with the recording wavelength is destructive. The diffraction efficiency η as function of exposure time for one cycle of real-time holographic exposure is shown schematically in fig. 1 [1].

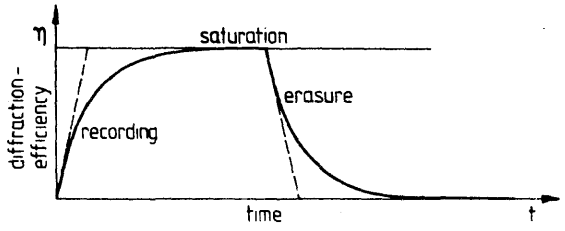

Fig. 1. Diffraction efficiency by recording and erasure.

2. Storage of speckle patterns in BSO crystal

Physical mechanisms for speckle pattern recording and erasure in BSO are drift and trapping of photoelectrons under illumination by a random light pattern field in the transverse electrooptic configuration. This gives

rise to a space-charge field which modulates the refractive index via the linear electrooptic effect. Erasure is achieved by space-charge relaxation under uniform illumination. Applying the double exposure technique, two speckle patterns are recorded whereby the second is shifted relative to the first due to an object displacement or tilt between the two exposures. Depending on the optical configuration speckle patterns for inplane displacement or tilt analysis can be recorded [6]. The two speckle patterns are separated by at least one speckle dimension, therefore the intensity of the speckle patterns is considered to perform a spatial modulation of energy density in the crystal. The two stored speckle patterns are illuminated by a plane or converging wave. In the Fraunhofer plane Youngs' fringes are modulating the diffraction halo displayed by the single speckle pattern. The fringe spacing is inversely proportional to the displacement.

For the crystals used the absorption coefficient was $\alpha_1 = 2\ \mathrm{cm}^{-1}$ for $\lambda_1 = 514$ nm and $\alpha_2 = 0.28\ \mathrm{cm}^{-1}$ for $\lambda_2 = 633$ nm. The speckle patterns were therefore recorded with light of the wavelength $\lambda_1 = 514$ nm and the Young's fringes displayed with $\lambda_2 = 633$ nm. The crystal thickness d was chosen to be 2.6 mm.

The intensity distribution of the speckle pattern imaged onto the BSO leads to a space-charge field, E_{sc}, by drift or diffusion of the photocarriers resulting in a refractive index variation. For speckles with dimensions $> 2\ \mu$m the space-charge field is proportional to the electric field, E_0, applied [3]. The refractive index modulation at saturation, Δn_s, can be written

$$\Delta n_s = n^3 r E_{sc}/2, \tag{1}$$

with n = refractive index ($n \simeq 2.5$ for $\lambda = 633$ nm), r = effective electrooptic coefficient, E_{sc} = space-charge field amplitude which is derived from Poissons equation [1].

The variation of the refractive index due to the speckle pattern can be written as

$$\Delta n = \Delta n_s\, C I'(u')/\langle I' \rangle \tag{2}$$

where $I'(u')$ is the intensity of the speckle pattern and $\langle I' \rangle$ the mean intensity. C is a constant taking into account the absorption in the crystal and reflection at the interface; it will be neglected. The recorded speckle pattern will now be illuminated with a wave of amplitude $A_0(u')$. The field amplitude considered to be immediately in front of the crystal will be written

$$A'(u') = A_0(u') \exp[(-\mathrm{i}2\pi/\lambda_1) d\, \Delta n], \tag{3}$$

λ_1 is the wavelength of recording and d is the crystal thickness. The photoinduced phase shift is small; $d\, \Delta n \ll \lambda_1$ (it is of the order of $\lambda_1/30$). The amplitude can therefore be written as

$$A'(u') \sim A_0(u') \left\{1 - \mathrm{i} \frac{2\pi}{\lambda_1} d\, \Delta n\right\}, \tag{4}$$

where the terms on the order of Δn^2 and higher are neglected. In eq. (4) it is assumed that the length of the speckles corresponds at least to the crystal thickness d. It was found experimentally that this requirement is not necessary.

In the following section, a short theoretical analysis of image plane speckle pattern recording in BSO crystals will be given.

3. Image plane speckle pattern recording in BSO crystals

A short theoretical analysis neglecting the crystal activity, birefringence and Bragg effect will be given to explain the fringe pattern obtained. The intensity of the speckle pattern in the image plane can be written as follows [6]

$$I(u') = \sum_q \sum_p \psi(x_p)\, \psi^*(x_q) \exp[\mathrm{i}2\pi\, u'(x_p - x_q)], \tag{5}$$

To simplify the writing the one-dimensional notation is used instead of a vector notation, according to fig. 2.

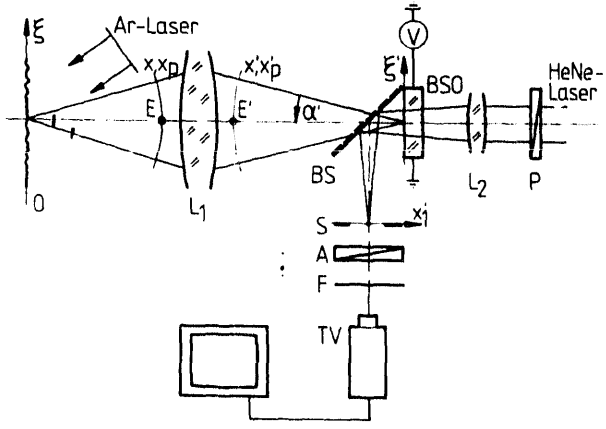

Fig. 2. Experimental arrangement for recording speckle patterns in the image plane and displaying Young's fringes.

u' = reduced coordinate; $u' = \frac{n \sin \alpha'}{\lambda} \xi'$

ξ' = rectangular coordinate in the image plane
α' = aperture angle in the image space
$x = x/h$, $x' = x'/h'$ = reduced coordinates in the entrance and exit pupil
h, h' = pupil heights
x_p, x_q = reduced coordinate in the entrance pupil plane
x_p', x_q' = reduced coordinate in the exit pupile plane
$\psi(x_p)$, $\psi^*(x_q)$ describe the optically rough surface and represent the angular components of the light scattered by the optically rough surface.

In the double exposure technique two speckle patterns are recorded in the crystal. The first is stored at nearly saturation and the second, the shifted, is recorded incoherently because the speckle separation is greater than the speckle size. For the second exposure of the displayed speckle pattern the original speckle pattern will not be affected very much. The intensity of the two speckle patterns recorded in the crystal is according to eq. (5) using one-dimensional notation

$$I(u', \Delta u') = C\left\{\sum_q \sum_p \psi(x_p)\, \psi^*(x_q) \times \exp[\mathrm{i}2\pi\, u'(x_p - x_q)] + \sum \sum \psi(x_p)\, \psi^*(x_q) \times \exp[\mathrm{i}2\pi(u' + \Delta u')\,(x_p - x_q)]\right\} \quad (6)$$

or by substituting x_r for $x_p - x_q$

$$I(u', \Delta u') = C\left\{\sum_q \sum_r \psi(x_r + x_q)\, \psi^*(x_q) \exp(\mathrm{i}2\pi\, u' x_r) + \sum_q \sum_r \psi(x_r + x_q)\, \psi^*(x_q) \times \exp[\mathrm{i}2\pi(u' + \Delta u')x_r]\right\}. \quad (7)$$

The double exposed speckle pattern leads to a refractive index variation in the crystal volume.

4. Displaying Young's fringes in the Fraunhofer plane

Illuminating the crystal with a coherent wave of wavelength λ_2 and absorption coefficient α_2 the wavefront emerging from the crystal can be written by neglecting Bragg volume effects in accordance with expressions (4)

$$A'(u') = A_0(u')\, C_1\left\{1 - \frac{\mathrm{i}\,2\pi}{\lambda} d\, \Delta n_s \frac{I(u', \Delta u')}{\langle I \rangle}\right\}, \quad (8)$$

where $A_0(u')$ represents the incident wave amplitude and C_1 is a constant, taking also into account the small absorption in the crystal for λ_2 and the reflection at the interface. For the analysis C_1 will be neglected and a plane wave of constant amplitude A_0 is considered. The Fourier transform in the focal plane is

$$a(x_1') = A_0 \int_{\text{crystal}} \left\{1 - \frac{\mathrm{i}2\pi}{\lambda_1} d\, \Delta n_s \frac{I(u', \Delta u')}{\langle I \rangle}\right\} \times \exp(\mathrm{i}2\pi x_1' u')\, \mathrm{d}u'$$

and the intensity is

$$|a(x_1')|^2 = A_0^2 \left\{\delta(x_1') + \left(\frac{2\pi}{\lambda_1} d\, \Delta n_s\right)^2 \times \left|\sum_q \frac{\psi(x_1' + x_q)\psi^*(x_q)}{\langle I \rangle}\right|^2 [1 + \cos 2\pi\, x_1' \Delta u']\right\}. \quad (9)$$

$\Delta n_s = (n^3 r\, E_{sc}/2)^2$

and $\Sigma_q\, \psi(x_1' + x_q)\, \psi^*(x_q)$ is the autocorrelation of the speckle in the pupil of the image forming lens.

The square of the autocorrelation of the exit pupil of the image forming lens is modulated by Young's interference fringes.

The in-plane displacement in the object plane is given by

$\Delta\xi = f_1' \lambda_2 / M\, x_c'$,

where f_1' = focal length or the distance from the crystal to the Fraunhofer-plane, depending on the experimental arrangement; M = lateral magnification; x_c' = fringe spacing.

For the fully illuminated pupil of the image forming lens, the radius of the autocorrelation is

$r_{x_1'} = 2 f_1' \sin \alpha'$.

Consequently, no fringes can be observed for $|x_1'| > r_{x_1'}$.

in the experiment it was found, however, that the fringe envelope is very often smaller. This may be due to the crystal thickness (Bragg effect) [8]. Furthermore, crystal activity and birefringence may influence the envelope of the Young's fringes.

A similar theory can be developed for tilt analysis by recording the speckle pattern in the Fourier transform plane of lens L_1 in fig. 2 [6] or in the image of the light source. In addition, the simplified theory can be extended to two dimensions.

5. Some experimental results

A typical experimental set-up for real time speckle pattern recording is shown in fig. 2 for displacement analysis. The optically rough surface was illuminated with an argon laser (λ_1 = 514 nm). The low aperture lens (NA = 0.06) formed the image in the crystal. The power on the crystal to write the speckle pattern was 15 μW cm^{-2} and the cycle time 1 s.

The BSO crystal was illuminated with a HeNe laser (1 mW) λ_2 = 633 nm. The Young's fringes were displayed in the Fraunhofer plane where a stop was placed to eliminate the undiffracted light; the fringes were observed on a TV screen. A dichroic beamsplitter BS reflects λ_2 and the analysator A reduces stray light [4,5]. Further details of the experimental arrangements will be described in a later paper.

In fig. 3 fringe patterns of displacements (fig. 3a) and tilts (fig. 3b) are observed. The object was a diffuse reflecting rough surface. The displacements were applied perpendicular to the applied field E_0 (4.8 kV) and tilts in a direction perpendicular to the first (f_1' = 90 mm).

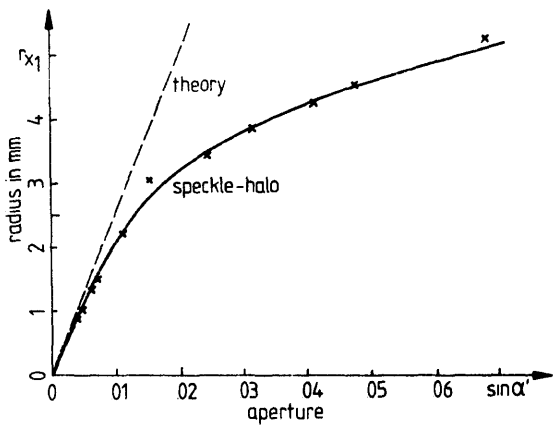

Fig. 4. Speckle halo plotted against the numerical aperture obtained with an arrangement corresponding to fig. 2.

In our analysis, the Bragg volume effect as well as crystal activity and birefringence were neglected. The experiments showed, however, that they can limit the speckle halo as shown in fig. 4 where the radius of the speckle halo $r_{x_1'}$ is plotted against the numerical aperture of lens L_1 in the image space. For small α' the autocorrelation of the pupil is limiting the halo as predicted. For larger α', however, the Bragg volume effect and the birefringence are probably limiting the field in which Young's fringes are observed.

6. Conclusions

Using BSO crystals in the transverse electrooptic-mode a real time operation of "speckle photography" techniques is achieved with unlimited recycling. The fringe analysis can be obtained directly using TV tech-

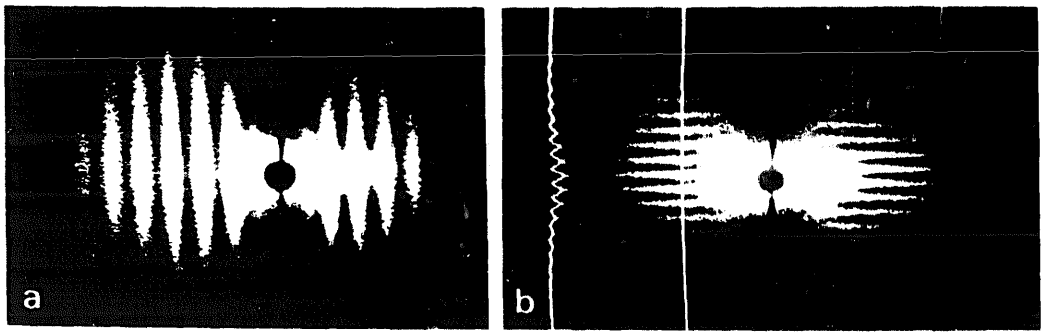

Fig. 3. Young's fringes obtained by a) an inplane displacement of 100 μm, b) a tilt of 25 sec of arc.

niques, as indicated in fig. 3b, where the fringe pattern is scanned directly. Further studies and applications are in preparation and will be reported.

We would like to thank J.P. Huignard and his colleagues for very helpful advice in handling the BSO crystals and the DFG for the financial support.

References

[1] J.P. Huignard and F. Micheron, Appl. Phys. Lett. 29 (1976) 591.

[2] J.P. Huignard, J.P. Herriau and T. Valentin, Appl. Optics 16 (1977) 2796;
J.P. Huignard and J.P. Herriau, Appl. Optics 16 (1977) 1897.

[3] J.P. Huignard, J.P. Herriau, G. Rivet and P. Günter, Optics Letters 5 (1980) 102.

[4] J.P. Herriau, J.P. Huignard and P. Auborg, Appl. Optics 17 (1978) 1851.

[5] M.P. Petrov, S.V. Miridonov, S.I. Stepanov, and V.V. Kulikov, Optics Comm. 31 (1979) 301.

[6] H.J. Tiziani, in: Speckle metrology, ed. R.K. Erf (Academic Press, 1978) p. 73.

[7] A.E. Ennos, in: Laser speckle and related phenomena, ed. J.C. Dainty (Springer, Berlin, 1975) p. 237.

[8] H. Kogelnik, Bell Syst. Techn. J. 48 (1969) 2909.